Experiments in Fluids 23 (1997) 217–224

The reduction of spatial aliasing by long hot-wire anemometer probes

J. H. Citriniti, W. K. George

Abstract Experiment and numerical analysis are presented to demonstrate that a hot-wire anemometer probe reduces spatial aliasing of turbulent velocity fluctuations because of the filtering property of the probe sensing element. The experiment focuses on the one-dimensional turbulent velocity spectrum and utilizes a long sensing length hot-wire probe to exaggerate the effect of the sensing element on the turbulent field. The numerical analysis utilizes a model of the hot-wire probe from Wyngaard (1968) along with isotropic turbulence relations to obtain an equation for the hot-wire response in a turbulent velocity field. The model can be used to determine the effect of hot-wire length on the one and three-dimensional turbulent spectra.

The experimental study demonstrates that the finite length, hot-wire probe filters out energy in the high wave number region of the one-dimensional spectrum thereby verifying its ability to reduce spatial aliasing. Interestingly, the study also shows that energy in the low wave numbers of the one-dimensional spectrum is attenuated. The numerical study of the hot-wire probe demonstrates that this low wave-number attenuation is purely an artifact of the one-dimensional spectrum and not an effect of the hot-wire probe.

List of symbols

α	Kolmogorov constant dimensionless
δ_{ij}	Kronecker delta dimensionless
ε	Isotropic dissipation [m^2/s^3]
$E(k)$	Spectrum function [m^3/s^2]
$F_{11}^1(k_1)$	One-dimensional, longitudinal, k_1-spectrum. Referred to as longitudinal, k_1-spectrum [m^3/s^2]
$F_{11}^2(k_2)$	One-dimensional, longitudinal, k_2-spectrum. Referred to as longitudinal, k_2-spectrum [m^3/s^2]
$\mathbf{k}$	Wave-number vector, $\mathbf{k}(k_1, k_2, k_3)$ [1/m]
k	Magnitude of wave-number vector, $k=(k_1^2+k_2^2+k_3^2)^{1/2}$, [1/m]
$\Phi_{ij}(\mathbf{k})$	Three-dimensional spectrum tensor [m^5/s^2]
$R_{\mathscr{L}}$	Reynolds number based on integral scale, $\mathscr{L}$ dimensionless
$S(f)$	Power spectral density of velocity signal output by hot wire probe [m^2/s]
$\mathbf{u}(\mathbf{x})$	Velocity vector [m/s]
$\hat{\mathbf{u}}(\mathbf{k})$	Fourier coefficient of transformed velocity vector [m/s]
^{m}	Superscript denoting a measured quantity, i.e., that output by the hot-wire probe or its analytical model

Received: 20 May 1996/Accepted: 14 November 1996

J. H. Citriniti
Department of Thermo and Fluid Dynamics,
Chalmers University of Technology,
S-412 96 Gothenburg, Sweden

W. K. George
Department of Mechanical and Aerospace Engineering
State University of New York at Buffalo
Buffalo, NY 14260, USA

Correspondence to: J. Citriniti

The authors wish to thank D. Ewing for his contributions to the numerical aspect of this paper. This work was funded by the National Science Foundation under grant number CTS 9102863 and was carried out in the Turbulence Research Laboratory at the State University of New York at Buffalo.

1 Introduction

Temporal aliasing of time signals has long been recognized and understood by experimentalists. In brief, aliasing occurs when information at higher frequencies is incorrectly placed in lower frequencies because the sampling rate is not high enough. Aliasing can be avoided if the sampling rate statistics satisfy the Nyquist criterion (Otnes and Enochson 1972), namely $f_s > 2f_N$, where f_s is the sampling rate and f_N is the highest frequency present in the data. If frequencies greater than (1/2) f_s exist in the data they must be removed by filtering to avoid aliasing.

A less recognized, and often overlooked, counterpart to temporal aliasing is produced by insufficient resolution of the *spatial* structure in a random field, i.e., spatial aliasing. A demonstration of spatial aliasing was presented by Glauser and George (1992) in an experimental study of the large scale structures in a turbulent, axisymmetric mixing layer. In their experiment, the two-point velocity correlation tensor determined at many positions in the mixing layer was decomposed into azimuthal Fourier modes. The velocity field was measured using hot-wire anemometers and the distribution of measuring positions in the azimuthal direction was varied to study the effects of spatial resolution on the decomposition. They found that the number of spatial measuring positions dramatically influenced the energy distribution within the azimuthal Fourier modes. Glauser and George were able to attribute

the difference between Fourier coefficients, calculated with different azimuthal spacing, to insufficient spatial resolution and a failure to satisfy the Nyquist criterion in space.

In the same paper, Glauser and George (1992) suggested that spatial aliasing could be reduced by using hot-wire probes with exceptionally long sensing elements. They claim that these long hot-wires are advantageous because their sensing elements act as a spatial filters that remove the high wave (or mode) number fluctuations. They suggested that the wire, in effect, acts as a spatial low-pass filter with a cut-off wavelength of $\lambda_c = 2\lambda_w$. This reduces spatial aliasing since it eliminates information in spatial scales with wavelengths λ_c, less than twice the wavelength of the wire, λ_w, i.e., those that cannot be resolved with a limited number of probes and whose information would consequently be aliased. This fact has been exploited in the experiment of Citriniti (1996) who used long hot-wires to reduce spatial aliasing of azimuthal modes in a round turbulent jet experiment.

The idea of removing high frequency fluctuations by averaging uniformly through sampling interval is not new, but has been applied only to time signals, see Kristensen (1971). There the Fourier transform of the signal being filtered is convolved with the transform of a uniform window. The result is that the spectrum of the sampled signal is related to that of the original signal by

$$S^m(f) = S(f)\left[\frac{\sin(\pi f \Delta t)}{\pi f \Delta t}\right]^2 \tag{1}$$

where Δt is the length of the sampling interval. Since space, unlike time, is three-dimensional, it is not immediately obvious if this technique can be applied to spatial averaging or even which spatial Fourier components of energy are removed by a single, long averaging element.

There have been numerous papers on the effect of spatial resolution on the measurement of small scales, but here the concern is with the large scales. In previous analyses spatial filtering was considered undesirable because it filtered structures which had information relevant to the experiment. Here, it is deliberately introduced to reduce information in these same scales before it is aliased. This paper, then, attempts to determine, both by experiment and theory, whether the long hot-wire probe can indeed reduce spatial aliasing.

2
Experiment

To investigate whether the long hot-wire probe could filter short wavelength scales in a turbulent field, an experiment was initiated which involved the measurement of a turbulent velocity field with (a) an extraordinarily long sensing length hot-wire probe and (b) three standard length hot-wire probes (see Fig. 1). The idea was to measure the effect of the probe sensing length on the turbulence by determining the turbulent velocity spectrum with the long wire and comparing it with the turbulent spectra obtained with the three short wires. Since the short wires measure the turbulent field to a much finer temporal and spatial scale, they are used to measure the true turbulent field, i.e., they provide baseline spectra with which to compare the long wire spectrum.

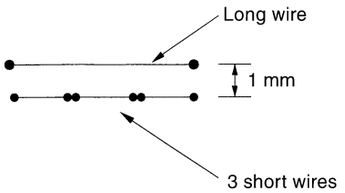

Fig. 1. Probe alignment in 4 wire experiment

2.1
Flow field

The turbulent velocity field used in this experiment was generated at the exit of an isothermal, round air-jet by attaching a wire mesh to the exit nozzle. The exit diameter of the jet[1] was 9.8 cm and the wire mesh was constructed with 16 threads per inch of 0.0254 cm stainless steel wire that produced a flow blockage of approximately 25%. The velocity of the fluid immediately downstream of the wire mesh was 16.9 m/s corresponding to a Reynolds number based on mesh thickness of 28000. Since the velocity profile leaving the jet exit is a top hat, the flow field generated by the wire mesh at the center of the jet exit is characterized as uniform, decaying turbulence and was found to have a turbulence intensity of 7.3%.

2.2
Experimental hardware

The three standard length wires had an $l/d = 200$ and the long wire had an $l/d = 2000$. The probes were positioned approximately 10 cm downstream of the mesh. The long wire was situated directly above the short wires approximately 1 mm away and since the flow field generated by the jet is uniform, each of the probes experiences nearly the same turbulent field. The 1 mm separation distance ensured that the probes were far enough apart so that no electrical cross contamination was experienced, see Perry (1982). The hot-wires were made of unplated, 12.7 μm tungsten wire (Sigmund-Cohn, Mt. Vernon, NY).

The sampling rate in this experiment was 18 kHz and the corner frequency of the phase matched, 8th order, anti-alias Bessel filters was 6 kHz for all probes. For each probe, 25 blocks of data with 2048 samples/block were recorded for a spectral bandwidth of 8.8 Hz. The individual blocks were separated by at least one integral scale so that each makes an independent contribution to the statistical calculations, see Tan-atichat and George (1985). The anemometers used in this experiment were made at SUNY Buffalo and are described in Citriniti et al. (1994).

2.3
Results of experiment

Figure 2 shows the one-dimensional spectra, F_{11}^1, as measured by the four probes. The data set with the filled box shows the turbulent velocity spectrum measured by the long sensing

[1]Described in Citriniti (1996)

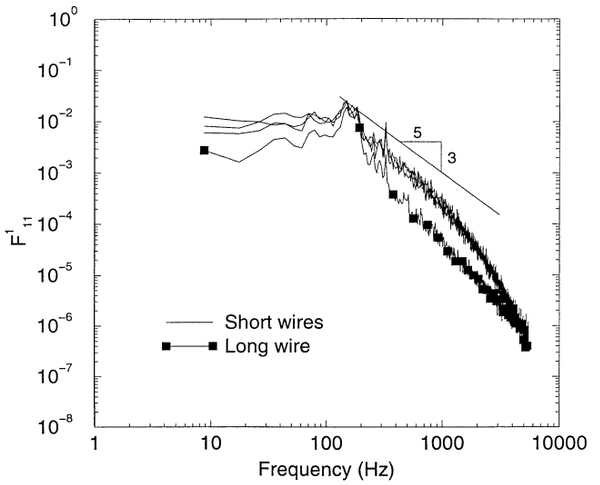

Fig. 2. Frequency spectrum of turbulence in 4 wire experiment

length hot-wire probe. The solid lines are the spectra obtained from the three short wires. Note that a fully developed turbulent field has been set up as demonstrated by the large $f^{-5/3}$ range.

As Fig. 2 shows, the spectral energy contained in the high frequencies of the long sensing length probe is 50% less than that of the short sensing length probes in the high frequency region. This effect is attributed to the filtering property of the long wire and demonstrates the ability of the probe to filter the short wavelength spatial scales in the flow.[2] Therefore, since the probe can filter the small scale fluctuations, it can be used to filter these scales out of the flow before the energy in them is aliased.

The long wire captures the energy containing portion of the spectrum ($f \approx 100$ Hz). This is important because it shows that the long wire does not attenuate the turbulence in the frequency range associated with a majority of the kinetic energy. Surprisingly, however, the energy in the low frequencies of the turbulent spectrum has been reduced by about 20%. This result, at first glance, appears to contradict the claims of Glauser and George (1992) who argue the energy attenuation by the long hot-wire probe should diminish as the frequency decreases. As will be shown in the next section, the reduced energy in the low frequencies of the long-wire spectrum in Fig. 2 is not caused by the long wire but by the use of the one-dimensional spectrum to present the results.

3
Theoretical analysis

To demonstrate that the low frequency roll-off in the spectrum of the long wire of Fig. 2 is a consequence of the one-dimensional spectrum and not an effect of the probe, a theoretical model of the long hot-wire was developed.

3.1
The hot-wire as a spatial filter

The hot-wire anemometer records a voltage signal that is proportional to the weighted-average of the fluid velocity along the sensing element of the probe. The velocity vector measured by a single hot-wire probe of length l can then be approximated as

$$\mathbf{u}^m(\mathbf{x}^m) = \frac{1}{l}\int_{x_2^m - l/2}^{x_2^m + l/2} \mathbf{u}(x_1^m, x_2, x_3^m)\, \mathrm{d}x_2 \tag{2}$$

where $\mathbf{u}^m$ is the velocity vector measured by the probe, $\mathbf{u}$ is the true velocity vector and $\mathbf{x}^m = (x_1^m, x_2^m, x_3^m)$ is the position of the center of the hot-wire probe (see Fig. 3). In Eq. (2) the probe is oriented parallel to the x_2 axis.

It is important to note the assumptions inherent in Eq. (2). First, note that Eq. (2) is just the convolution of the velocity vector with the wire sampling window which in this case is a top hat. Other wire sampling windows could be used, such as parabolic or exponential distributions, but they are not considered in this analysis. Second, it is implicitly assumed that the wire responds uniformly to velocity perturbations along its length, i.e., no non-linear effects caused by large velocity gradients in the fluid are included in this analysis. This discussion then obviously excludes flows with strong mean shear or high turbulence intensities where severe velocity gradients could exist locally along the probe sensing element. However, it should be noted that this is an implied assumption for any proper implementation of the hot-wire anemometer probe, since operating them in such conditions invalidates the transducer calibration and therefore the voltage to velocity conversion.

Representing the integral of Eq. (2) in Fourier space and manipulating yields (Wyngaard 1968),

$$\mathbf{u}^m(\mathbf{x}^m) = \int \int_{-\infty}^{\infty} \int \hat{\mathbf{u}}(\mathbf{k}) \exp(\mathrm{i}\mathbf{k}\cdot\mathbf{x}) \left[\frac{1}{l}\int_{-l/2}^{l/2} \exp(\mathrm{i}k_2 x_2)\, \mathrm{d}x_2\right] \mathrm{d}\mathbf{k} \tag{3}$$

where $\mathbf{k} = (k_1, k_2, k_3)$ is the wave number vector and $\hat{\mathbf{u}}$ are the Fourier coefficients of the true velocity vector. It is assumed that the turbulence is homogeneous so that the flow field can be represented using Fourier transforms in the sense of generalized functions (Lighthill 1956).

The solution to the integral within the brackets of Eq. (3) is straightforward and, after evaluating the limits using the Euler

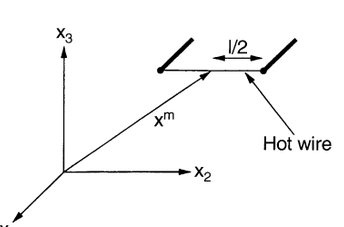

Fig. 3. Hot-wire anemometer probe orientation for analytical analysis

[2]The probe can only filter spatial scales but the consequences of this appears in the frequency spectrum via Taylor's hypothesis, see Wyngaard (1968)

formula for sin x, gives,

$$\mathbf{u}^m(\mathbf{x}^m) = \int_{-\infty}^{\infty} \int \hat{\mathbf{u}}(\mathbf{k}) \exp(i\mathbf{k}\cdot\mathbf{x}) \left[\frac{\sin(k_2 l/2)}{k_2 l/2}\right] d\mathbf{k} \quad (4)$$

Thus, the velocity measured by the probe is a product of the true velocity and an attenuation factor (shown in the brackets). This factor can be thought of as a spatial filter that has been imposed by the finite length of the probe and its magnitude decreases from unity as its argument, in this case $k_2 l/2$, increases. What this means in Eq. (4) is that the apparent contribution to the velocity vector of any Fourier coefficient is no longer $\hat{\mathbf{u}}(\mathbf{k})$ but rather

$$\hat{\mathbf{u}}(\mathbf{k}) \left[\frac{\sin(k_2 l/2)}{k_2 l/2}\right]$$

and thus the measured velocity vector contains less information in the higher wave numbers than is truly present in the field. This result is identical to the time filter described earlier, see Eq. (1), except that $\hat{\mathbf{u}}(\mathbf{k})$ is a vector argument instead of a scalar.

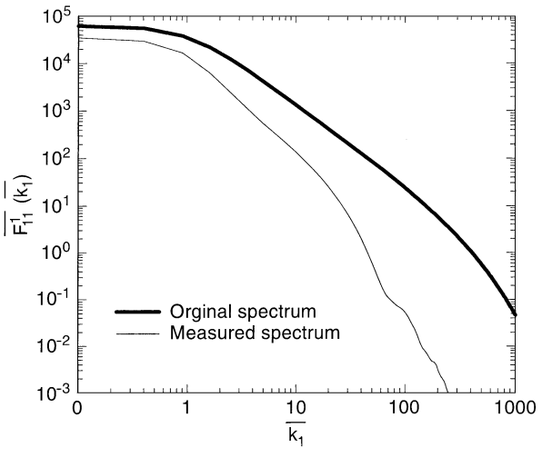

Fig. 4. Non-dimensional, longitudinal spectra, $\overline{F_{11}^1}(\overline{k_1})$ and $\overline{F_{11}^{1m}}(\overline{k_1})$

3.2 Velocity statistics

Typically, it is not the velocity itself which is of interest, but rather the two-point correlation and its Fourier transform, the spectrum. The one-dimensional form of the longitudinal k_1-spectrum can be defined by

$$F_{11}^1(k_1) = \int_{-\infty}^{\infty} \Phi_{11}(k_1, k_2, k_3)\, dk_2\, dk_3 \quad (5)$$

where Φ_{11} is the streamwise form of the three-dimensional spectrum tensor,[3] Φ_{ij}. Using generalized functions, one can derive the corresponding longitudinal k_1-spectrum as measured by the hot-wire, see Appendix A,

$$F_{11}^{1m}(k_1) = \int_{-\infty}^{\infty} \Phi_{11}(\mathbf{k}) \left[\frac{\sin(k_2 l/2)}{k_2 l/2}\right]^2 dk_2\, dk_3 \quad (6)$$

which models the effects of finite length hot-wire probes on turbulent velocity spectra. This model shows that the one-dimensional spectrum is indeed low-pass filtered by the probe and energy is removed from wave-numbers above the corner frequency, $k_2 \approx 1/l$, at least in the direction aligned with the probe.

3.3 Numerical solution method

A numerical solution to Eq. (6) can be formulated once a model for the three dimensional spectrum tensor, Φ_{ij}, is provided. If the turbulent field is assumed isotropic, the spectrum tensor can be written as (Batchelor 1953)

$$\Phi_{11}(\mathbf{k}) = \frac{E(k)}{4\pi k^2}\left(1 - \frac{k_1^2}{k^2}\right) \quad (7)$$

where k is the magnitude of the wavenumber vector $\mathbf{k}$ and $E(k)$ is the spectrum function.

Closure of the equation requires a model for the spectrum function, $E(k)$. Pao (1965) developed a model for $E(k)$ that contains the exponential roll off characteristic of the high wave number part of the spectrum. A model which is useful in the low wave number region of the spectrum was developed by Von Kármán (1948) and Helland et al. (1977) combined these two to create a spectrum function that models both large and small wave number fluctuations.

The Helland et al. (1977) spectrum function can be non-dimensional by the isotropic dissipation, ε, and the integral scale in the flow, $\mathscr{L}$, to give,[4]

$$\bar{E}(\bar{k}) = \alpha (R_{\mathscr{L}})^{5/4} \left(\frac{\bar{k}_1}{\bar{k}}\right)^4 \left[1 + \left(\frac{\bar{k}_1}{\bar{k}}\right)^2\right]^{-17/6} \exp\left[-\frac{3\alpha}{2R_{\mathscr{L}}}\left(\frac{\bar{k}_1}{\bar{k}}\right)^{4/3}\right] \quad (8)$$

where $\bar{k}_1 = k_1 \mathscr{L}$ is the non-dimensional wave number in the k_1 direction, $R_{\mathscr{L}} = u\mathscr{L}/\nu$ is the turbulent Reynolds number and $\bar{k} = k_1/k$, where the over-bar denotes non-dimensional quantities. The Kolmogorov constant, α, was chosen to be 1.6.

The longitudinal k_1-spectrum can be non-dimensionalized in a similar manner to yield,

$$\bar{F}_{11}^1(\bar{k}_1) = \int_0^{2\pi} \int_0^1 \frac{\bar{E}(\bar{k})}{4\pi\bar{k}} (1 - \bar{k}^2)\, d\bar{k}\, d\theta \quad (9)$$

where θ is a parameter created by the non-dimensionalization. The first integral in Eq. (9) can be integrated to obtain

$$\bar{F}_{11}^1(\bar{k}_1) = \frac{1}{2}\int_0^1 \frac{\bar{E}(\bar{k})}{\bar{k}} (1 - \bar{k}^2)\, d\bar{k} \quad (10)$$

[3]The notation used follows that of Tennekes and Lumley (1972) with the superscript, n on F_{ij}^n representing the direction normal to the plane of integration

[4]The parameter $\mathscr{L}$ is not actually the integral scale in the flow but rather a function of it, but for the quantitative aspects of this study it is taken as the integral scale

and the corresponding equation for the measured spectrum is

$$\bar{F}_{11}^{1m}(\bar{k}_1) = \int_0^{2\pi} \int_0^1 \frac{\bar{E}(\bar{k})}{4\pi\bar{k}} (1-\bar{k}^2) \left[\frac{\sin(z)}{z}\right]^2 \mathrm{d}\bar{k}\, \mathrm{d}\theta \qquad (11)$$

where $z = \bar{k}_1 \bar{l} \cos\theta/(2\bar{k})$ and $\bar{l} = l/\mathscr{L}$ is the non-dimensional wire length. Equations (10) and (11) were solved with the use of Eq. (8) using a Gauss–Legendre quadrature method.

3.4 Results

The original, longitudinal k_1-spectrum, corresponding to Eq. (10), and the measured spectrum, given by Eq. (11), are shown in Fig. 4. As expected, there is less energy in the measured one-dimensional spectrum at the high wave numbers than is present in the original turbulent field. This is a direct result of the attenuation factor in Eq. (11) and is the numerical counterpart to the high frequency filtering performed by the long hot-wire in the experimental aspect of this study. However, another interesting feature in Fig. 4 is the behavior of the measured spectrum in the low wave number region. The difference between the original and measured spectra at the low wave numbers is essentially the same as that obtained by the experimental part of this analysis, see Sect. 2.

At low wave numbers the true one-dimensional spectrum should be recovered by the long hot-wire because the model for the spatial attentuation factor (see Eq. (11)) approaches unity as the wave number approaches zero. Figure 4 suggests that this is not the case. To explain this low frequency (and low wave-number) effect, the three-dimensional spectrum must be utilized.

4 Wave-number and spatial aliasing in turbulent spectra

4.1 Three-dimensional spectrum

For isotropic turbulence, surfaces of constant energy for the streamwise, three-dimensional spectrum tensor, $\Phi_{11}(\mathbf{k})$, are shaped like toroids. A shell of constant energy in the *measured* three-dimensional spectrum tensor, $\Phi_{11}^m(k)$, is shown as the gray surface in Fig. 5. The measured three-dimensional spectrum tensor is determined in the same manner as the measured one-dimensional spectrum tensor, see Sect. 3.2. The light areas on the plane slicing through the shell represents energy in the *original*, three-dimensional spectrum tensor, Φ_{11}.

When the slicing plane is $k_2 = 0$ there is no light emanating from the plane indicating that the measured and original three-dimensional spectra are equivalent at that wave number. As the plane moves down the x_2 axis (the direction aligned with the hot-wire probe in our model, see Fig. 3) the probe filtering begins to attenuate the measured three-dimensional spectrum, thus more light is emitted from the slicing plane. As the plane moves further down the k_2 axis more and more light is emitted indicating greater attenuation by the probe.

Figure 5 illustrates several important points:

1. The hot-wire probe attenuates energy in the three-dimensional spectrum in the direction aligned with the probe sensing element.
2. Information in the low wave numbers of the three dimensional spectrum is properly recovered by the transducer.
3. The probe attenuation increases as the wave number gets larger (relative to the wire length).

4.2 Probe attenuation in one-dimensional spectrum

Point number 2 above states that there is no energy attenuation by the hot wire probe at the low wave numbers of the three-dimensional spectrum. The question then is; why does the measured one-dimensional spectrum appear to show probe attenuation in the same frequency and wave-number range, see Figs. 2 and 4? The answer to this question lies in the definition of the one-dimensional spectrum. This point is discussed in Chap. 8 of Tennekes and Lumley (1972) and is the essence of wave-number aliasing.

Recall that the original, longitudinal k_1-spectrum, $F_{11}^1(k_1)$, is defined by the integral in Eq. (5) and the spectrum obtained from a transducer in the same turbulent field by Eq. (6). These equations demonstrate that F_{11}^1 is simply the integral of the three-dimensional spectrum tensor over planes perpendicular to the k_1 direction. In Fig. 6 the light area on the slicing plane is a visual representation of this spectrum, at each wave number. The area bounded by the gray shell lying on the cutting plane in this figure must then represent the longitudinal k_1-spectrum as measured by the transducer, $F_{11}^{1m}(k_1)$. In the first part of the figure the cutting plane is at $k_1 = 0$ and at this wave number the measured, longitudinal k_1-spectrum is smaller than the original spectrum as indicated by the light areas on the cutting plane, i.e., $F_{11}^{1m}(0) < F_{11}^1(0)$. This is a direct result of the hot-wire probe filtering in the k_2 direction, i.e., the direction aligned with the probe. Thus, even at $k_1 = 0$ there is a difference between the measured and original longitudinal k_1-spectra.

This fact explains the difference between the original and measured spectra in the low frequencies of the experimental part of this paper, see Sect. 2 and Fig. 2, and in the one-dimensional spectra of the numerical work, see Sect. 3.4. and Fig. 4. In essence, wave-number aliasing, an unavoidable consequence of the one-dimensional spectrum, has created a region in the low frequencies (and low wave-numbers) in which the energy in the spectrum is reduced. It is important to realize that this is not a result of the transducer, but rather a manifestation of aliasing in the calculation of the one-dimensional spectrum.

4.3 Effect of wire length

In a different presentation of probe filtering, Fig. 7 shows the three-dimensional spectrum where the effect of the wire length has been added. In this figure, the gray surface is a constant-energy contour of the original three-dimensional spectrum tensor, Φ_{11}. The blue shading on the surface represents wave number combinations in which the energy in the measured three-dimensional spectrum tensor, Φ_{11}^m, equals that in the original spectrum. For a very short sensing length (e.g., a probe length to integral scale ratio of 0.01) the measured and original three-dimensional spectra are identical, hence the blue shading nearly covers the entire gray shell when $l/\mathscr{L} = 0.01$. As the wire length normalized by the integral scale increases ($l/\mathscr{L}$ gets

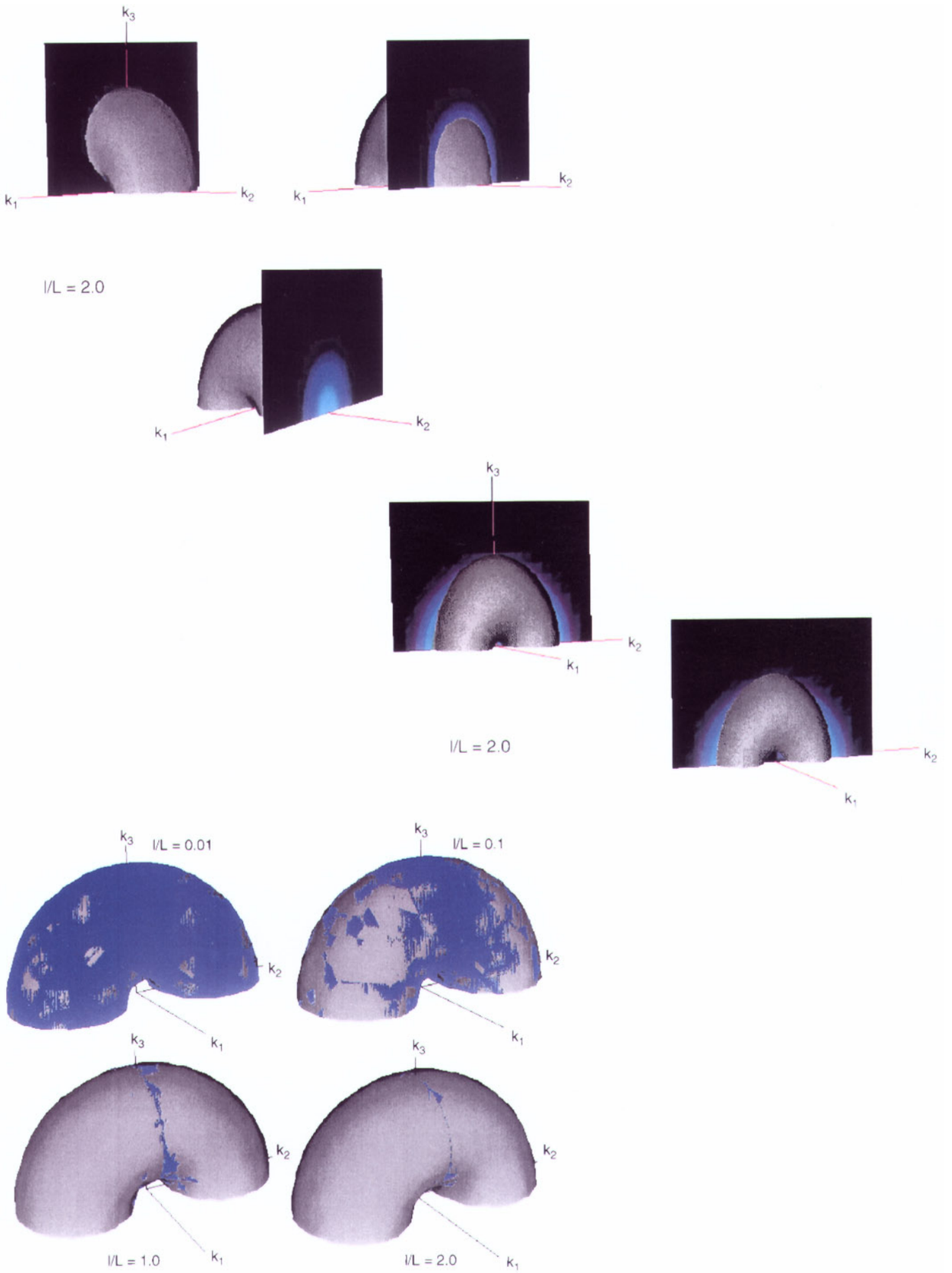
k3
k1
k2
k3
k1
k2
l/L = 2.0
k3
k1
k2
k3
k1
k2
l/L = 2.0
k3
l/L = 0.01
k2
k1
k3
l/L = 0.1
k2
k1
k3
k2
k1
l/L = 1.0
k3
k2
k1
l/L = 2.0

larger) the attenuation of the three-dimensional spectrum increases along the x_2 axis and consequently the amount of blue shading decreases in that direction. As the wire length is increased further a large portion of the spectrum is attenuated. However, note that the blue shading is always present at $k_2 = 0$. This indicates that the original three-dimensional spectrum is always recovered at the smallest wave numbers, independent of the probe sensing length. In other words, *the statistics of the turbulence at low wave numbers are properly recovered by the long hot-wire probe.*

5 Conclusions

The analyses presented in this work have shown that the long hot-wire anemometer probe can be used to reduce spatial aliasing by using the spatial filtering property of the probe to remove the small scale turbulent fluctuations which contribute to spatial aliasing. The first part of the paper demonstrated this filtering property experimentally by using a long hot-wire probe to exaggerate the effect of the probe on the turbulent field.

A limitation of the presentation technique, i.e., the one-dimensional spectrum, suggested that the probe may affect the large scale turbulent structure in some way. The numerical analysis of Sect. 3 showed that this affect was a result of wave-number aliasing in the one-dimensional spectrum and therefore independent of the hot-wire probe. In this respect, the one-dimensional spectrum was found to be a misleading investigative device. A more useful measure of the hot-wire probes effect on the turbulence was accomplished using the three-dimensional spectrum, which is free from effects of wave-number aliasing.

The results of the numerical analysis showed that the filtering of spatial scales by the hot-wire probe occurred in the direction aligned with the probe sensor and the amount of attenuation increased with probe sensor length. An estimate of the probe attenuation can be obtained using the analytical model in Eq. (4) (see Citriniti and George 1996). Finally, the analyses presented in this paper are not limited to hot-wire anemometers but are applicable to any measuring device which integrates thermodynamic effects over space, e.g., shear stress sensors, pressure transducers, see Lueptow (1995), or LDA, see Buchhave et al. (1979).

Fig. 5. Three-dimensional spectrum for a fixed wire length of 2 times the integral scale in the flow. The gray surface is the measured, isotropic three-dimensional spectrum tensor and the blue shading on the cutting plane represents the energy in the original, isotropic spectrum tensor at a single wavenumber. The cutting plane represents $\bar{F}^2_{11}$

Fig. 6. Three-dimensional spectrum for fixed wire length. See Fig. 5 for extended caption. Cutting plane represents $\bar{F}^1_{11}$

Fig. 7. Three-dimensional spectrum for various wire lengths. The gray surface is a contour of the original, isotropic three-dimensional spectrum. The blue shading represents points of equivalent energy in the measured, isotropic three-dimensional spectrum

Appendix A: Measured one-dimensional spectrum

The one-dimensional spectrum, $F^1_{ij}(\mathbf{k})$ can be defined in terms of the three dimensional spectrum tensor, $\Phi_{ij}(\mathbf{k})$,

$$F^1_{ij}(\mathbf{k}) = \int_{-\infty}^{\infty}\int_{-\infty}^{\infty} \Phi_{ij}(\mathbf{k})\, \mathrm{d}k_2\, \mathrm{d}k_3 \tag{A.1}$$

and the corresponding measured one-dimensional spectrum is

$$F^{1m}_{ij}(\mathbf{k}) = \int_{-\infty}^{\infty}\int_{-\infty}^{\infty} \Phi^m_{ij}(\mathbf{k})\, \mathrm{d}k_2\, \mathrm{d}k_3 \tag{A.2}$$

For homogeneous turbulence, Monin and Yaglom (1975) have shown that non-overlapping, Fourier coefficients in the three-dimensional spectrum are uncorrelated so that

$$\Phi_{ij}(\mathbf{k})\,\delta(\mathbf{k}-\mathbf{k}') = \overline{\hat{\mathbf{u}}(\mathbf{k})\,\hat{\mathbf{u}}^*(\mathbf{k}')}\, \mathrm{d}\mathbf{k}\, \mathrm{d}\mathbf{k}' \tag{A.3}$$

and analogously,

$$\Phi^m_{ij}(\mathbf{k})\,\delta(\mathbf{k}-\mathbf{k}') = \overline{\hat{\mathbf{u}}^m(\mathbf{k})\,\hat{\mathbf{u}}^{m*}(\mathbf{k}')}\, \mathrm{d}\mathbf{k}\, \mathrm{d}\mathbf{k}' \tag{A.4}$$

The analysis of Sect. 3.1 has shown that the Fourier coefficients of the measured velocity field are attenuated by the probe, i.e.,

$$\hat{\mathbf{u}}^m(\mathbf{k}) = \hat{\mathbf{u}}(\mathbf{k}) \left[\frac{\sin(k_2 l/2)}{k_2 l/2}\right] \tag{A.5}$$

and substituting this into Eq. (A.4) yields,

$$\Phi^m_{ij}(\mathbf{k})\,\delta(\mathbf{k}-\mathbf{k}') = \overline{\hat{\mathbf{u}}(\mathbf{k}) \left[\frac{\sin(k_2 l/2)}{k_2 l/2}\right] \hat{\mathbf{u}}^*(\mathbf{k}') \left[\frac{\sin(k_2 l/2)}{k_2 l/2}\right]}\, \mathrm{d}\mathbf{k}\, \mathrm{d}\mathbf{k}' \tag{A.6}$$

where the probe is again oriented in the x_2 direction. The bracketed terms can be removed from the ensemble average to obtain,

$$\Phi^m_{ij}(\mathbf{k})\,\delta(\mathbf{k}-\mathbf{k}') = \left[\frac{\sin(k_2 l/2)}{k_2 l/2}\right]^2 \underbrace{\overline{\hat{\mathbf{u}}(\mathbf{k})\,\hat{\mathbf{u}}^*(\mathbf{k}')}\, \mathrm{d}\mathbf{k}\, \mathrm{d}\mathbf{k}'} \tag{A.7}$$

where the underbrace represents the unfiltered three-dimensional spectrum tensor and substituting Eq. (A.3) produces,

$$\Phi^m_{ij}(\mathbf{k}) = \Phi_{ij}(\mathbf{k}) \left[\frac{\sin(k_2 l/2)}{k_2 l/2}\right]^2. \tag{A.8}$$

Finally, the equation for the measured one-dimensional spectrum, provided in Sect. 3.2, is determined through substitution into Eq. (A.2)

$$F^{1m}_{ij}(\mathbf{k}) = \int_{-\infty}^{\infty}\int_{-\infty}^{\infty} \Phi_{ij}(\mathbf{k}) \left[\frac{\sin(k_2 l/2)}{k_2 l/2}\right]^2 \mathrm{d}k_2\, \mathrm{d}k_3. \tag{A.9}$$

References

Batchelor GK (1953) Homogeneous turbulence. Cambridge: Cambridge University Press

Buchhave P; George WK; Lumley JL (1979) The measurement of turbulence with the laser-doppler anemometer. In: van Dyke, Wehausen, and Lumley (editors) Ann Rev Fluid Mech 11: 443–503. Academic Press, Palo Alto, CA

Citriniti JH; George WK (1996) Experimental investigation into the dynamics of the axisymmetric jet mixing layer. In: Begell, W. (editor) Turbulence, Heat and Mass Transfer, New York, NY. Begell House

Citriniti JH; Taulbee KD; Woodward SH; George WK (1994) Design of multiple channel hot wire anemometers. In: Fluid Measurement and Instrumentation 1994, pp 67–73, ASME FED-Vol. 183

Citriniti JH (1996) Experimental investigation into the dynamics of the axisymmetric mixing layer utilizing the proper orthogonal decomposition. PhD thesis, State University of New York at Buffalo

Glauser MN; George WK (1992) Application of multipoint measurements for flow characterization. Exp Thermal Fluid Sci 5: 617–632

Helland KN; Van Atta CW; Stegen GR (1977) Spectral energy transfer in high reynolds number turbulence. J Fluid Mech 70: 337–359

Kristensen L (1971) The effect of aliasing, averaging and smoothing in digital spectral analysis. In: Kjelaas, A.G. (editor) Statistical Methods and instrumentation in geophysics, pp 1–24. Teknologisk Forlag, Oslo, Norway

Lighthill MJ (1956) An introduction to Fourier analysis and generalized functions. Cambridge: Cambridge University Press

Leuptow RM (1995) Transducer resolution and the turbulent wall pressure spectrum. J Acoust Soc Am 97(1): 370–378

Von Kármán T (1948) Progress in the statistical theory of turbulence. In: Pro Nat Acad Sci 34: 530–539

Monin AS; Yaglom AM (1975) Statistical fluid mechanics Vol. I and II. Cambridge: MIT Press

Otnes RK; Enochson L (1972) Digital time series analysis. New York: Wiley

Pao YH (1965) Structure of turbulent velocity and scalar fields at large wave numbers. Phys Fluids 8: 1063–1075

Perry AE (1982) Hot Wire Anemometry. Oxford: Clarendon Press

Tan-atichat J; George WK (1985) Handbook of fluids and fluid machinery, Use of Computers in Data Acquisition. New York: Wiley

Tennekes H; Lumley JL (1972) A First course in Turbulence. Cambridge: The MIT Press

Wyngaard JC (1968) Measurement of small-scale turbulence with hot wires. J Scientific Instruments 1: 1105–1108